




RESEARCH ARTICLE OPEN ACCESS

Functional Link Between *IRC7* Allelic Variation and Carbon-Sulfur- β -Lyase Activity in Brewing *Saccharomyces cerevisiae* Strains

C. Nasuti¹ | V. Papiani Ceramelli¹ | D. Tagliazucchi²  | A. Cattivelli²  | L. Solieri¹ 

¹Lactic Acid Bacteria and Yeast Biotechnology (LYB) Lab, Department of Life Sciences, University of Modena and Reggio Emilia, Via Amendola 2 42122, Reggio Emilia, Italy | ²Nutritional Biochemistry Lab, Department of Life Sciences, University of Modena and Reggio Emilia, Via Amendola 2 42122, Reggio Emilia, Italy

Correspondence: L. Solieri (lisa.solieri@unimore.it)

Received: 28 July 2025 | **Revised:** 27 February 2026 | **Accepted:** 2 March 2026

Academic Editor: Anupama Bose

Keywords: β -lyase | beer thiols | brewing yeasts | *IRC7* gene | L-cysteine | S-ethyl-L-cysteine | S-methyl-L-cysteine

ABSTRACT

The *IRC7* gene encodes a β -lyase enzyme critical for the release of volatile thiols during beer fermentation, contributing to aroma development in fermented beverages. In this study, 15 *Saccharomyces cerevisiae* ale brewing strains were analyzed to investigate *IRC7* allelic diversity and its functional implications. Using a nested PCR approach combined with sequencing, three genotypes were identified: *IRC7^L/IRC7^L*, *IRC7^L/IRC7^S*, and *IRC7^S/IRC7^S*. Allelic segregation in two sporulation-competent heterozygous strains was achieved through spore dissection and haplo-selfing, enabling the generation of homozygous monosporic derivatives. In total, 18 *IRC7* sequences were characterized, including 15 *IRC7^L* alleles carrying different combinations of 9 amino acid substitutions and 3 truncated *IRC7^S* variants. Two substitutions previously associated with reduced enzymatic activity, G101D and T185A, were frequently detected in *IRC7^L* alleles. Protein stability predictions indicated a destabilizing effect of these mutations, and sequence similarity analysis highlighted substantial variability among closely related *IRC7^L* variants. In vitro β -lyase activity assays performed using three model substrates (L-cysteine, S-ethyl-L-cysteine, and S-methyl-L-cysteine) showed that strains carrying *IRC7^L* generally exhibited higher enzymatic activity, while the presence of the *IRC7^S* allele or the T185A substitution in *IRC7^L* allele was associated with reduced activity in a substrate-dependent manner. Monosporic derivatives confirmed that the *IRC7^S* allele markedly impairs β -lyase activity and that T185A negatively affects activity toward S-methyl-L-cysteine. Overall, these findings expand the current knowledge of *IRC7* genetic and functional diversity in brewing strains and its implications for flavor development. The results provided a basis for implementing genotype-informed yeast selection, whereas the mating-competent monosporic derivatives carrying *IRC7^L* allele generated in this study represent valuable resources for future breeding strategies aimed at optimizing thiol release and aroma complexity in beer.

1 | Introduction

Beer is the third most consumed beverage in the world after water and tea, and consumer demand for novel beers with an expanded aromatic profile is steadily increasing [1]. Within the

brewing industry, the rapid expansion of the craft beer sector has promoted the exploration of diverse beer styles and the adoption of innovative production strategies aimed at enhancing sensory complexity [2]. Central to these developments is the role of yeast,

This is an open access article under the terms of the [Creative Commons Attribution](https://creativecommons.org/licenses/by/4.0/) License, which permits use, distribution and reproduction in any medium, provided the original work is properly cited.

Copyright © 2026 C. Nasuti et al. *Journal of Food Biochemistry* published by John Wiley & Sons Ltd.

which not only converts fermentable sugars into ethanol during fermentation but also contributes decisively to the aroma and flavor of the final product.

Saccharomyces cerevisiae ale strains are major producers of flavor-active secondary metabolites, including higher alcohols and esters such as 2-phenylethanol, isoamyl acetate, and ethyl hexanoate, which arise as byproducts of alcoholic fermentation [3–5]. Beyond *de novo* synthesis of these compounds, yeasts also modulate beer aroma through the biotransformation of non-volatile precursors derived from malt and hops. Among them, polyfunctional thiols are of particular importance due to their extremely low sensory thresholds and their ability to impart desirable fruity, citrus, tropical fruit, or black- and white-currant notes to beer and other fermented beverages [6–8].

Polyfunctional thiols are present predominantly as odorless cysteine- or glutathione-bound precursors in malted barley and hops [9]. During fermentation, yeast cells uptake cysteinylated conjugates through the Gap1 permease, while glutathionylated forms are transported through the Opt1 transporter. One internalized, these conjugates are enzymatically cleaved to release volatile, aroma-active thiols [10, 11]. In *Saccharomyces cerevisiae*, at least three genes (*IRC7*, *STR3*, and *CYS3*) encode cysteine-S-conjugate-lyase enzymes capable of breaking carbon–sulfur bonds and releasing volatile sulfur compounds [1, 11]. *STR3* and *CYS3* encode a peroxisomal cystathionine β -lyase (EC 4.4.1.13) and a cytoplasmic cystathionine γ -lyase (EC 4.4.1.1), respectively, which have been shown to contribute only marginally to the thiol release [12–14]. In contrast, *IRC7* gene encodes a cytosolic cystathionine β -lyase (EC 4.4.1.8) of approximately 400 amino acids that functions as a homotetramer and represents the major determinant of thiol release from cysteinylated precursors. This enzyme is responsible for the liberation of key aroma compounds such as 4-mercapto-4-methylpentan-2-one (4-MMP) and 3-mercaptohexan-1-ol (3-MH) [12, 13, 15]. Deletion of *IRC7* resulted in significant reductions in both 4-MMP (~96%) and 3-MH (~40%), largely independent of the initial cysteinylated precursor availability [12, 13, 15–17]. These thiols impart characteristic grapefruit-like and passionfruit-like notes that are highly valued in fermented beverages [16, 18, 19].

Extensive genetic diversity within the *IRC7* locus has been documented in wine yeast populations and has been shown to underlie strain-dependent variability in thiol-releasing capacity [20]. A well-characterized polymorphism consists of a 38-bp deletion that introduces a premature stop codon, shortening the protein length from 400 to 340 amino acids [19, 21, 22]. This truncated form, referred to as *IRC7^S*, encodes a nonfunctional β -C-S lyase, in contrast to the fully active enzyme encoded by the full-length *IRC7^L* allele. Wine strains carrying *IRC7^S* exhibit significantly reduced production of 3-MH and 4-MMP compared with strains carrying *IRC7^L* when grown in synthetic grape juice medium [19]. Additional point mutations may co-occur within both *IRC7^S* and *IRC7^L* alleles and further contribute to the wide variability in the β -lyase activity observed across wine yeast population. Among them, the A553G nucleotide substitution causes a threonine-to-alanine change at position 185 (T185A), which disrupts the binding site of pyridoxal 5'-phosphate co-factor and significantly impairs β -lyase activity [19]. In addition to sequence polymorphisms, changes in *IRC7* copy number have

been associated with differences in thiol release, with increased gene dosage correlating with enhanced β -lyase activity [23].

Because *Irc7* activity generates intracellular accumulation of pyruvate-, ammonium-, and sulfur-containing metabolites, *IRC7* gene expression is tightly regulated by the nitrogen catabolite repression (NCR) pathway, which prioritizes the utilization of preferred nitrogen sources [24]. Under nitrogen-rich conditions, genes involved in the assimilation of secondary nitrogen sources are repressed, whereas their expression is derepressed upon depletion of preferred nitrogen compounds [25]. Within this regulatory pathway, *URE2* acts as a key repressor of *IRC7* transcription and mutations affecting *URE2* or related regulatory genes result in derepression of *IRC7* expression and enhanced thiol release [26, 27].

Recent population-level studies have revealed that the *IRC7^S* allele in homozygous state is prevalent in wine yeast populations and positively linked to several advantageous phenotypes, including oxidative stress resistance, copper tolerance, and improved growth performance in grape must [17, 21]. Specifically, unfunctional *IRC7^S* gene increases intracellular cysteine availability, favoring the synthesis of glutathione, an important antioxidant that enhances yeast fitness under enological stress conditions [19]. Furthermore, *IRC7* expression is downregulated in high copper concentrations, a condition frequently encountered in grape juice, likely due to its involvement in cysteine homeostasis [28]. Together, these findings suggest that *IRC7^S* may represent a signal of domestication within the wine yeasts, favoring traits beneficial for winemaking, despite its reduced aroma contribution.

In contrast to wine yeasts, comparatively little is known about *IRC7* allelic diversity and its functional consequences in brewing yeasts. Although recent studies have begun to address this topic [9, 21, 23], comprehensive biochemical and genetic analyses remain limited. Therefore, this study aims to characterize the genotypic and phenotypic diversity of *IRC7* in 15 industrial *S. cerevisiae* ale brewing strains. Specifically, *IRC7* allelic variation was investigated, β -lyase activity was quantified in vitro using three model substrates, and genotype–phenotype correlations were evaluated to elucidate the contribution of *IRC7* variants to the production of brewing-relevant aroma compounds.

2 | Materials and Methods

2.1 | Strains and Culture Conditions

Fifteen industrial *S. cerevisiae* ale brewing strains provided by AEB Brewing (Brescia, Italy) were included in this study (Table 1). Strains were routinely cultivated on YPD medium (1% yeast extract, 2%, peptone 2% dextrose), supplemented with 2% agar when required, at 27°C for 24 h and conserved at 4°C for the duration of experiments. For long-term storage, isolates were preserved at –80°C containing 25% (v/v) glycerol as a cryoprotectant. Sporulation efficiency and spore viability were assessed according to the methods described in [29].

2.2 | *IRC7* Gene Characterization

Genomic DNA from yeast strains was extracted according to Hoffman and Winston [30]. Characterization of *IRC7* gene was

TABLE 1 | *Saccharomyces cerevisiae* ale brewing strains used in this study and their associated phenotypic and genetic features.

Strain code	% Sporulation	% Spore viability	MAT genotype	IRC7 genotype
ale1	—	NA	MATa/MAT α	IRC7 ^S /IRC7 ^L
ale2	48	0	MATa/MAT α	IRC7 ^L /IRC7 ^L
ale3	—	NA	MATa/MAT α	IRC7 ^L /IRC7 ^L
ale4	46.3	39	MATa/MAT α	IRC7 ^L /IRC7 ^L
ale5	—	NA	MATa/MAT α	IRC7 ^L /IRC7 ^L
ale6	—	NA	MATa/MAT α	IRC7 ^L /IRC7 ^L
ale7	24.7	0	MATa/MAT α	IRC7 ^L /IRC7 ^L
ale8	50	46	MATa/MAT α	IRC7 ^S /IRC7 ^S
ale9	—	NA	MATa/MAT α	IRC7 ^L /IRC7 ^L
ale10	—	NA	MATa/MAT α	IRC7 ^L /IRC7 ^L
ale11	27.3	52.9	MATa/MAT α	IRC7 ^S /IRC7 ^L
ale12	48	0	MATa/MAT α	IRC7 ^L /IRC7 ^L
ale13	—	NA	MATa/MAT α	IRC7 ^L /IRC7 ^L
ale14	87	37	MATa/MAT α	IRC7 ^S /IRC7 ^L
ale15	—	NA	MATa/MAT α	IRC7 ^L /IRC7 ^L

Note: IRC7^S denotes the short IRC7 allele, whereas IRC7^L denotes the long IRC7 allele, as established by the nested PCR assay. Abbreviation: NA, not applicable.

performed using the primer sets described by Roncoroni et al. [15]. Primers were detailed in Supporting Table S1. Specifically, full-length PCR amplification of IRC7 gene was carried out with the primer pair PF7/PR8. To detect the presence of the truncated gene version IRC7^S, a nested PCR assay was performed using the internal primer pair PF2/PR2. For both PCR assays, *S. cerevisiae* strain US-05 (Fermentis, Lesaffre, France), which carries the long variant of the IRC7 gene (IRC7^L) (GCA_019155645.1), was used as a positive control. All PCR reactions performed were carried out with Phusion High-Fidelity DNA Polymerase (Cat. No. F530S, Thermo Scientific, Waltham, USA), following the manufacturer's instruction. PCR amplicons were resolved by electrophoresis on a 1.8% (w/v) agarose gel stained with ethidium bromide (5 μ g/mL). The GeneRuler 100 bp Plus DNA Ladder (Cat. No. SM0321 Thermo Scientific, Waltham, USA) or the GeneRuler 100 bp DNA Ladder (Cat. No. SM0241 Thermo Scientific, Waltham, USA) was used as a molecular size marker. DNA fragments were visualized under UV transillumination, and gel images were captured using a Gel Doc imaging system (Bio-Rad, Hercules, CA, USA).

2.3 | Tetrad Dissection and Cloning Procedure

For sporulating heterozygous IRC7^L/IRC7^S strains, segregation of the two allelic variants was assessed through tetrad dissection followed by the generation of monosporic cultures (MSCs), as previously described [31]. Briefly, heterozygous IRC7^L/IRC7^S yeasts were grown on YPD plates at 28°C for 24 h and subsequently transferred on acetate agar medium (1% sodium acetate, 2% agar) to induce sporulation. After incubation at 27°C for 4–6 days, asci were collected and treated with 0.2 mg/mL of Zymolyase 20T (Seikagaku Corporation, Japan) for 15 min at room temperature to partially digest the ascus cell wall. The resulting asci suspension was streaked onto YPDA plates, and tetrad dissection was performed using a micromanipulator (Singer Instruments, Somerset, UK). Plates were incubated at 28°C

for 48 h to allow MSC colony formation. All MSCs were subjected to at least one round of purification prior to subsequent analyses.

For nonsporulating strains, full-length PCR amplicons were cloned into the pJET plasmid using the CloneJET PCR Cloning kit (Cat. No. K1231, Thermo Scientific, Waltham, MA, USA), following the manufacturer's instructions. The resulting plasmid was used to transform *Escherichia coli* DH10B chemically competent cells (Cat. No. EC0113, Thermo Scientific, Waltham, MA, USA). Transformed colonies were selected on Luria-Bertani medium supplemented with 100 μ g/mL of ampicillin. Plasmid DNA was extracted using the GeneJET Plasmid Miniprep Kit (Cat. No. K0502, Thermo Scientific, Waltham, MA, USA), according to the manufacturer's protocol.

2.4 | MAT Genotyping

MAT genotyping was carried out on brewing strains and their MSCs using the primers described by Huxley et al. [32]. Strains BY4742 (MAT α) and BY4743 (MATa/MAT α) were purchased from Euroscarf and used as internal controls. PCR mixtures were performed with DreamTaq Green DNA Polymerase (Cat. No. EP0712, Thermo Scientific, Waltham, MA, USA), and primers are detailed in Supporting Table S1.

2.5 | Phylogenetic and Statistical Analysis

Direct Sanger sequencing of full-length PCR amplicons was performed using both PF7 and PR8 primers. For amplicons cloned into the pJET plasmid, sequencing was carried out using the pJET_Fw and pJET_Rv primers (Supporting Table S1). Contig sequences were merged using the program SeqMan (DNASTAR, Madison, WI, USA), and poor-quality ends were edited manually to remove primers. The multiple sequence alignment of the deduced Irc7 amino acid sequences was computed using MUSCLE [33]. When required, the alignments

were visualized with Jalview v2.11.2.5 [34]. The phylogenetic tree was constructed using the maximum likelihood method and Whelan–Goldman WAG model [35] of amino acid substitution. *Irc7* amino acid sequences from strains AWRI1631 (EDZ72363.1), YJM789 (EDN59205.1), S288C (NP_116714.1), and VL3 (EGA87043.1) were retrieved from NCBI database (accessed in January 2025).

All the phylogenetic analyses were carried out using MEGA 11 software program [36]. Sequences were deposited in the GenBank database under accession numbers PV876887–PV876904.

2.6 | Molecular Modeling Analysis

Prior to structural modeling, the frequencies of amino acid substitutions were calculated to assess both the overall mutation rates and the prevalence of individual mutations across the analyzed yeast strains. A predictive functional assessment was subsequently performed to estimate the potential impact of each amino acid substitution on *Irc7* function. Changes in protein stability associated with each mutation were then predicted by calculating the variation in Gibbs free energy ($\Delta\Delta G$) using the I-Mutant2.0 tool from the BioFold platform (<https://folding.biofold.org/i-mutant/i-mutant2.0.html>). In this framework, negative $\Delta\Delta G$ values indicate a destabilizing effect on protein structure, whereas positive $\Delta\Delta G$ values suggest increased stability [37]. All $\Delta\Delta G$ predictions were based on the primary amino acid sequence of the *Irc7* protein. The algorithm evaluated protein stability under constant conditions of temperature (25°C) and pH (7.0).

2.7 | Biochemical and Phenotypic Assays

The specific enzymatic activity of each strain was determined spectrophotometrically using L-cysteine (Cat. No. 1028380100), S-ethyl-L-cysteine (Cat. No. S361615), and S-methyl-L-cysteine (Cat. No. M6626) as substrates (all from Sigma-Aldrich St. Louis, MO, USA), following the protocol described by Cordente et al. [19], with minor modifications.

Briefly, yeast strains were precultured in 20 mL of YPD medium at 26°C for 24 h under shaking conditions (150 rpm). Following incubation, a volume corresponding to 1×10^8 CFU was centrifuged at $4000 \times g$ for 5 min, under refrigerated conditions. The resulting cell pellet was washed with sterile distilled water, prior to mechanical lysis. Cells were resuspended in 198 μ L of breaking buffer (100 mM Tris-Cl, pH 6.8, containing 2% v/v Triton X-100), supplemented with 100 mM phenyl-methylsulfonyl fluoride (PMSF) (Cat. No. P7626, Sigma-Aldrich St. Louis, MO, USA). Approximately 50 μ L of sterile acid-washed glass beads (425–600 μ m) (Cat. No. G8772, Sigma-Aldrich St. Louis, MO, USA) were added, and samples were subjected to four cycles of vortexing for 4 min at 4°C, alternating with 4 min on ice, to ensure efficient cell disruption and release of intracellular and membrane-bound proteins, including the *Irc7* enzyme.

Following the lysis, samples were centrifuged at $8000 \times g$ for 5 min at 4°C to recover the crude cell extract. Aliquots of the supernatant (lysate) were collected and stored on ice.

Protein concentrations were assessed using the Bradford protein assay [38]. Absorbance was measured at 595 nm with a microplate reader (Multiskan, Thermo Scientific, USA), and values were determined by comparison to a calibration curve generated

from serial dilutions of bovine serum albumin (Cat. No. A941, Sigma-Aldrich St. Louis, MO, USA).

To measure β -lyase enzymatic activity, a volume of 50 μ L of lysate sample was added to 950 μ L of reaction mixture containing 1 mM of substrate, 20 μ M pyridoxal 5'-phosphate (Cat. No. 82870, Sigma-Aldrich St. Louis, MO, USA), 16.6 mM phosphate buffer, and 0.83 mM EDTA (pH 7). After a 60 min incubation at ambient temperature, the reaction mixture was supplemented with 2 μ L of L-lactate dehydrogenase (LDH; EC 1.1.1.27; Cat. No. L2625, Sigma-Aldrich St. Louis, MO, USA) and 100 μ L of a 3 mM NADH solution (Cat. No. 10128023001, Sigma-Aldrich St. Louis, MO, USA). The enzymatic conversion of pyruvate to lactate by LDH consumes NADH, which is oxidized to NAD^+ . The decrease in absorbance at 340 nm was measured at $t = 0$ min and $t = 30$ min to quantify NADH consumption. This decrease is stoichiometrically related to the amount of pyruvate formed and, therefore, reflects the β -lyase activity.

Data were expressed as the specific enzymatic activity (mU/mg) and calculated according to the following equation:

$$\text{specific activity (U/mg)} = \frac{\Delta A \times V_{\text{tot}} \times \text{Dilution factor}}{\epsilon \times l \times t \times [\text{Protein}]}, \quad (1)$$

where ΔA = change in absorbance at 340 nm between $t = 0$ and $t = 30$; V_{total} = total reaction volume (in mL); dilution factor = if the sample was diluted before the assay; ϵ = molar extinction coefficient (in $\text{M}^{-1} \text{cm}^{-1}$) of the product or substrate; l = path length of the cuvette (usually 1 cm); t = time (in minutes) over which ΔA is measured; and $[\text{protein}]$ = concentration of the total protein in the assay (mg/mL).

The capability to release aromatic thiol compounds was also assessed microbiologically by plating 10-fold dilutions of cell suspensions on BiGGY (Bismuth Glucose Glycine Yeast) agar medium [39].

2.8 | Statistical Analyses

All assays were performed in triplicate, and statistical analyses were carried out with GraphPad Prism v10 (GraphPad Software, San Diego, CA, USA). Differences in β -lyase activity among individual strains were assessed using one-way ANOVA ($p < 0.05$). Differences in β -lyase activity among the four *IRC7* genotypes were evaluated using the nonparametric Kruskal–Wallis test. Where significant differences were observed ($p < 0.05$), groupwise comparisons were subsequently analyzed with the Mann–Whitney U test. Nonparametric tests were applied for genotype-based comparisons due to unequal group sizes and non-normal data distribution.

3 | Results and Discussion

3.1 | Screening for Short and Long *IRC7* Allelic Variants

Although in *S. cerevisiae* the *STR3* and *CYS3* genes encode carbon–sulfur β -lyase enzymes and have been positively linked to thiol formation [12, 14], the *IRC7* gene is considered the primary responsible for the release of the major polyfunctional thiols such as 4-MMP and 3-MH. According to Belda et al. [17], the gene coding for this protein can be present in a longer form or a short form, depending on the strain and only the long allelic variant

IRC7^L encodes a fully active enzyme. Consequently, a nested PCR approach was employed to amplify the full-length *IRC7* gene in 15 *S. cerevisiae* commercial ale brewing strains. This assay enabled discrimination between the *IRC7^S*, carrying the 38 bp-long indel, and the *IRC7^L* allelic variant, as previously described [15, 19].

Full-length PCR amplification was successfully obtained for all 15 strains analyzed, yielding PCR amplicons of approximately 2000 bp (Supporting Figure S1, panel A). Subsequent nested-PCR using the internal primer PF2 and PR2 enabled the differentiation of brewing strains into three genotypic categories (Table 1). Three strains (ale11, ale1, and ale14) were tentatively identified as *IRC7^L/IRC7^S* heterozygotes, based on the presence of two PCR amplicons of approximately 432 and 394 bp (Supporting Figure S1, panel B). One strain (ale8) displayed a single amplicon of app. 394 bp and was identified as homozygous *IRC7^S/IRC7^S*. The remaining 11 strains displayed a single 432 bp-long band and were classified as homozygous *IRC7^L/IRC7^L* (Supporting Figure S1, panel B).

Direct sequencing of PCR amplicons was successfully obtained for both *IRC7^L/IRC7^L* and *IRC7^S/IRC7^S* homozygous strains, whereas it failed for the heterozygous *IRC7^L/IRC7^S* strains (ale11, ale1, and ale14), as expected due to overlapping allelic sequences. Notably, the predominance of the *IRC7^L* allele in homozygosity among the brewing strains contrasts sharply with observations in wine yeast populations, in which the functional *IRC7^L* allele has been reported at a much lower frequency in the homozygous state (approximately 5%–15%) [21].

3.2 | Segregation of Long and Short Variants in Heterozygous *IRC7^L/IRC7^S* Brewing Strains

In an effort to segregate the *IRC7^S* and *IRC7^L* allelic variants present in heterozygous strains, we generated their homozygous derivatives by exploiting meiosis and haplo-selfing (Figure 1(a)). Haplo-selfing refers to the ability of homothallic haploid yeasts to mate their first daughter cell by mating-type switching, leading to diploid derivatives, which are homozygous at all loci except the mating type (*MAT*) locus [40, 41]. This approach requires heterozygous strains to undergo sporulation under carbon source starvation and to produce viable spores. Accordingly, sporulation efficiency and meiotic spore viability were first evaluated for the three heterozygous strains (Table 1). Strains ale11 and ale14 successfully sporulated and underwent meiosis under carbon-starved conditions, producing a viable progeny with efficiencies of 52.9% and 37%, respectively, and were therefore suitable candidates for allele segregation via spore dissection. In contrast, strain ale1 was able to sporulate but failed to produce viable spores (Table 1).

For strain ale11, 22 asci were dissected, and 7 viable MSCs were recovered and screened using the *IRC7*-targeting nested-PCR approach described above. Only MSCs carrying the *IRC7^L* allele were obtained, whereas no MSCs harboring *IRC7^S* were recovered. In contrast, for strain ale14, MSCs containing either the long or short *IRC7* allelic variant were successfully isolated (Figure 1(b)).

To assess whether MSCs of strain ale11 and ale14 had undergone haplo-selfing, selected MSCs were genotyped for mating type. As

shown in Figure 2, MSCs from both parental strains displayed either *MATa/MATa* or *MATa* profile. This result suggests that the original parental strains ale11 and ale14 may be *HO/ho* heterozygotes, such that the gametes inheriting the *ho* allele are heterothallic and lack the ability to switch mating type. Depending upon the ploidy of the parental strains, MSCs harboring *MATa* genotype could represent haploids derived from diploid parents or *MATa/MATa* diploids derived from tetraploid parents. In both cases, *MATa* MSCs carrying a single functional *IRC7^L* allele are of particular interest, as they are mating-competent and may be directly exploited in future yeast breeding programs.

For strain ale1, which was unable to sporulate (Table 1), an alternative approach was employed to separate the *IRC7* allelic variants. The *IRC7* amplicon was cloned into *E. coli*-competent cells, and individual clones were screened using the nested PCR described above. Clone_06 yielded a nested PCR fragment of 394 bp, corresponding to the *IRC7^S* variant, whereas clone_07 yielded a nested PCR amplicon of 432 bp, corresponding to the *IRC7^L* variant (Supporting Figure S2). Based on the PCR product size, clone_06 and clone_07 were selected for subsequent sequencing. Alignment of the deduced amino acid sequences showed that clone_06 harbored the truncated *IRC7^S* allele, while clone_07 carried the full-length *IRC7^L* allele (Supporting Figure S3), thereby validating the successful cloning of both allelic variants.

3.3 | Sequencing, Molecular Modeling, and Phylogenetic Analysis

Globally, 18 *IRC7* sequences were obtained in this study: 13 directly from brewing strains, 3 through the constitution of MSCs, and 2 through a cloning strategy. Translation of these sequences yielded 18 deduced Irc7 amino acid variants, three of which carried the premature codon stop responsible for the truncated form of Irc7^S protein. In addition to the truncating mutation, nine further amino acid substitutions were identified among the long Irc7 variants (Table 2), highlighting a substantial level of sequence diversity within the brewing-associated *S. cerevisiae* strains considered in this study.

To investigate the potential impact of missense mutations on Irc7 protein stability and function, changes in $\Delta\Delta G$ were predicted using I-Mutant 2.0. Negative $\Delta\Delta G$ values indicate a decrease in protein stability, while positive values suggest enhanced stability. For this analysis, the protein sequence of the YJM789 strain was used as the reference, as it carries the long Irc7 variant without the T185A substitution and is therefore considered to represent the most catalytically active form of the enzyme (Table 3). In most cases, the predicted $\Delta\Delta G$ values were consistent with the expected functional effects. For instance, the mutation G101D and T185A provided the negative $\Delta\Delta G$ and were predicted to be deleterious consistently with previous studies [19, 21].

For S27T, which has been predicted to be functionally neutral, the negative $\Delta\Delta G$ may result from the different steric hindrance introduced by threonine compared to that of serine (Table 3). Similarly, the reduced stability predicted for the F55L substitution could be plausibly attributed to the replacement of the bulky benzene ring of phenylalanine with the smaller aliphatic side chain of leucine, potentially affecting local protein packing

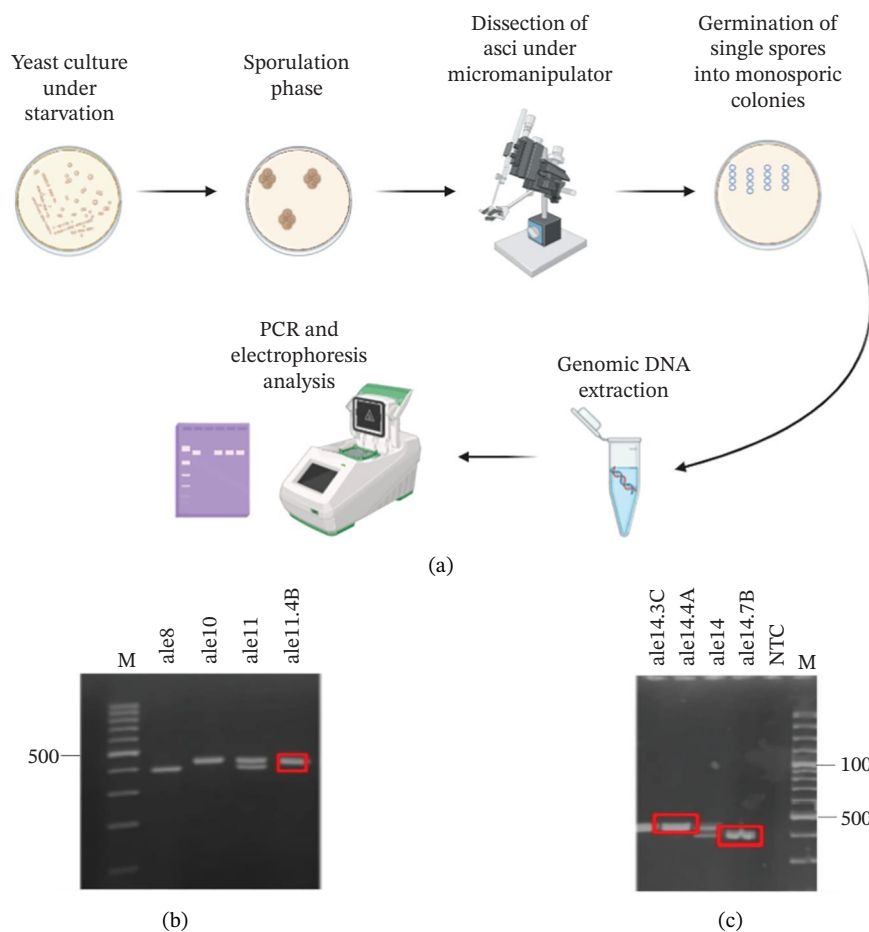


FIGURE 1 | Genotyping of *IRC7* allelic variants in monosporic cultures (MSCs) obtained from sporulating-competent, heterozygous *IRC7^L/IRC7^S* brewing strains. (a) Schematic workflow showing the isolation of MSCs from heterozygous strains capable of sporulation. The procedure includes sporulation induction, tetrad dissection via micromanipulation, and isolation of single-spore colonies for subsequent genotyping. The panel was generated using BioRender (<https://www.biorender.com>, accessed on June 8, 2025). (b) Nested PCR analysis of the heterozygous strain ale11, showing a double band indicative of the *IRC7^L/IRC7^S* genotype, and the MSC ale11.4A, which displays a single band indicative of *IRC7^L* allele. Strains ale8 and ale10 were used as *IRC7^S/IRC7^S* and *IRC7^L/IRC7^L* homozygous controls. (c) Nested PCR analysis of the heterozygous strain ale14, exhibiting a double band indicative of the *IRC7^L/IRC7^S* genotype, along with MSCs ale14.3C (*IRC7^L*), ale14.4A (*IRC7^L*), and ale14.7B (*IRC7^S*). Abbreviations: M, DNA ladder used as a molecular size marker; fragment length is in bp.

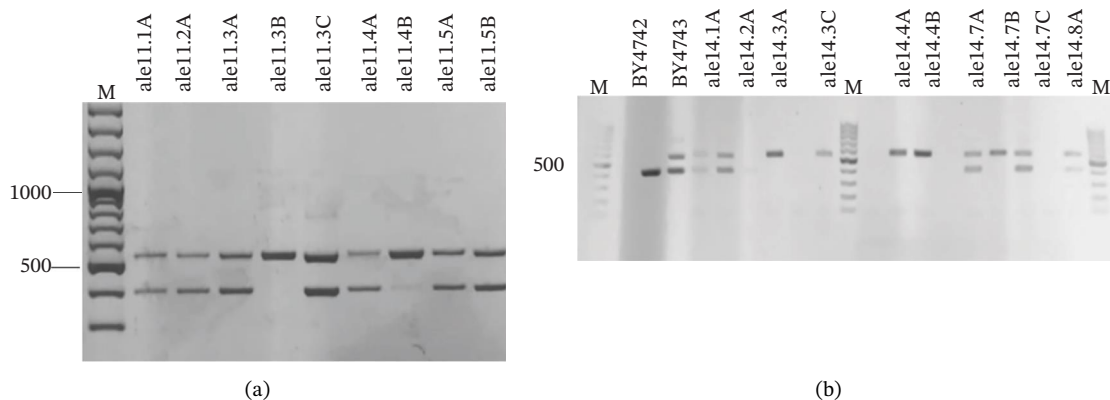


FIGURE 2 | *MAT* locus genotyping of monosporic clones (MSCs) obtained from the heterozygous *IRC7^L/IRC7^S* brewing strains ale11 (a) and ale14 (b). MSCs of parental strain ale11 carried only *IRC7^L*, whereas MSCs of parental strain ale14 carried either *IRC7^L* or *IRC7^S* allele. *S. cerevisiae* BY4741 (*MAT α*) and BY4743 (*MAT α /MAT α*) were used as controls. M, DNA ladder used as a molecular size marker; fragments length is in bp.

TABLE 2 | Summary of amino acid changes identified in the 18 *Irc7* variants across 15 brewing *Saccharomyces cerevisiae* strains.

Strain	Genotype	Amino acid positions									
		27	49	55	77	101	146	185	341	348	356
ale1_clone06	<i>IRC7^S</i>	S	E	F	G	G	A	T	X	NA	NA
ale1_clone07	<i>IRC7^L</i>	S	E	L	G	G	P	A	Y	V	A
ale2	<i>IRC7^L</i>	S	E	F	G	D	P	A	Y	V	A
ale3	<i>IRC7^L</i>	S	E	F	G	G	P	T	Y	L	A
ale4	<i>IRC7^L</i>	S	E	F	G	G	P	T	Y	V	A
ale5	<i>IRC7^L</i>	S	Q	F	G	G	P	A	Y	V	A
ale6	<i>IRC7^L</i>	S	E	F	G	G	P	T	Y	L	A
ale7	<i>IRC7^L</i>	S	E	F	G	D	P	A	Y	V	V
ale8	<i>IRC7^S</i>	S	E	F	G	G	P	T	X	NA	NA
ale9_var1	<i>IRC7^L</i>	S	E	F	G	G	P	A	Y	V	V
ale9_var2	<i>IRC7^L</i>	S	E	F	G	D	P	A	Y	V	V
ale10	<i>IRC7^L</i>	S	E	F	G	G	P	T	Y	V	A
ale11_4B	<i>IRC7^L</i>	T	E	F	G	G	P	A	Y	V	A
ale12	<i>IRC7^L</i>	S	E	F	S	D	P	A	Y	V	A
ale13	<i>IRC7^L</i>	S	E	F	G	G	P	A	Y	V	A
ale14_4A	<i>IRC7^L</i>	S	E	F	G	G	P	A	Y	V	A
ale14_7B	<i>IRC7^S</i>	S	E	F	G	G	P	T	X	NA	NA
ale15	<i>IRC7^L</i>	S	E	F	G	D	P	A	Y	V	V
VL3	<i>IRC7^L</i>	S	E	F	G	G	P	A	Y	V	A
YJM789	<i>IRC7^L</i>	S	E	F	G	G	P	T	Y	V	A
S288c	<i>IRC7^S</i>	S	E	F	G	G	P	T	X	NA	NA
AWRI1631	<i>IRC7^S</i>	S	E	F	G	G	P	A	X	NA	NA

Note: *Irc7* proteins from VL3, YJM789, S288c, and AWRI1631 were retrieved from GenBank and used as references. "X" indicates the introduction of a stop codon.

(Table 2). These observations suggest that even mutations predicted to be neutral at the functional level may contribute cumulatively to structural variability in *Irc7* proteins.

The most frequent deleterious substitution was T185A, which was identified in 12 out of 18 deduced *Irc7* proteins (Figure 3). The second most frequent deleterious mutation was G101D, which was exclusively observed in strains carrying the *IRC7^L* allele. This mutation has been reported to severely impair *Irc7* activity in wine yeasts [19]. Notably, strain ale9, initially classified as homozygous *IRC7^L/IRC7^L*, displayed a heterozygous nucleotide position, which resulted in G101D substitution (Table 2). This finding indicates that ale9 harbors two distinct *IRC7^L* alleles, one of which carries the G101D change (*IRC7^{L,G101D}*), further increasing the allelic complexity observed among brewing ale strains.

Interestingly, none of the truncated *Irc7^S* proteins carried either the T185A or the G101D mutation, suggesting that the combination of a premature stop codon with either of these two mutations may have been subject to counterselection (Table 2). The only point mutation identified in the deduced *Irc7^S* variants was P146A, which was detected in the cloned *IRC7^S* allele of the heterozygous strain ale1. This substitution was predicted to be functionally neutral by i-Mutant (Table 3). Notably, position 146 has also been reported as a mutational hotspot in wine yeast strains, where the P146R substitution is frequently observed [19].

Phylogenetic analysis of the 15 *Irc7* long protein variants revealed the presence of three main groupings, although branch support was generally low, indicating limited phylogenetic resolution. One grouping comprised strains carrying the potentially deleterious T185A mutation, whereas the second one included the strains lacking the T185A substitution. The third grouping consisted of strains harboring T185A in combination with additional mutations, including the deleterious G101D and the neutral A356V substitutions. Given the weak bootstrapping support, there was no robust phylogenetic separation among these groupings, which should not be interpreted as well-resolved evolutionary lineages. Nevertheless, the analysis underscores the high degree of sequence variability among *IRC7^L* proteins, as most brewing strains exhibited unique combinations of point mutations (Figure 4(a)). This diversity suggests ongoing diversification at the sequence level, which may contribute to strain-specific differences in the β -lyase enzymatic activity.

When considering only the mutations experimentally validated as deleterious by Cordente et al. [19], namely, T185A substitution and the truncating deletion responsible for the *Irc7* short form, 10 theoretical genotypic combinations can be defined. However, only four combinations were observed among 15 ale brewing strains considered in this study: *IRC7^L_T/IRC7^L_T*, *IRC7^L_A/IRC7^L_A*, *IRC7^S_T/IRC7^S_T*, and *IRC7^L_A/IRC7^S_T* (Figure 4(b)). Notably, the *IRC7^S* allele was consistently

TABLE 3 | Predicted stability and functional impact of point mutations in Irc7 proteins.

SNP	% Incidence	Type of substitution	Predicted functional effect	$\Delta\Delta G$
S271*	6.6%	Conservative (polar \rightarrow polar)	Likely neutral	-1.34
F55L*	6.6%	Conservative (hydrophobic \rightarrow hydrophobic)	Likely neutral	-1.82
E49Q*	6.6%	Nonconservative (negatively charged \rightarrow polar)	Potentially deleterious (affects charge interactions)	-0.13
G77S	6.6%	Nonconservative (hydrophobic \rightarrow polar)	Potentially deleterious	-1.34
G101D	33.3%	Nonconservative (hydrophobic \rightarrow negatively charged)	Deleterious	-1.43
P146A*	6.6%	Conservative (polar \rightarrow polar)	Likely neutral	-1.46
T185A	60%	Nonconservative (polar \rightarrow hydrophobic)	Deleterious (disrupts PLP binding)	-2.06
V348L	6.6%	Conservative (hydrophobic \rightarrow hydrophobic)	Likely neutral	-1.45
A356V	20%	Conservative (hydrophobic \rightarrow hydrophobic)	Likely neutral	1.01

Note: The table summarizes the single nucleotide polymorphisms (SNPs) identified in the analyzed brewing strains, including their frequency (%), type of amino acid substitution (conservative or nonconservative), the predicted functional effect based on biochemical properties, and the predicted $\Delta\Delta G$ values (kcal/mol) calculated using I-Mutant2.0. Negative $\Delta\Delta G$ values indicate a decrease in protein stability, while positive values suggest increased stability. Asterisk indicates non-synonymous mutations not previously detected in [22].

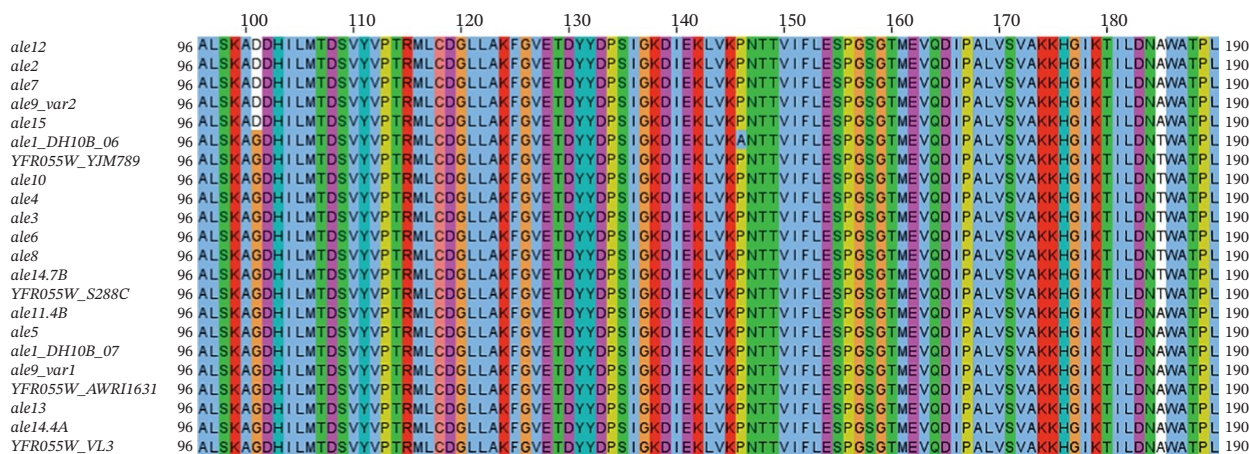


FIGURE 3 | Partial alignment of 18 *Irc7* deduced amino acid sequences obtained from 15 brewing strains. For brevity, the figure depicts only 94 amino acid residues from position 96 to position 190. *Irc7* amino acid sequences of reference strains VL3, AWRI1631, S288c, and YJM789 were retrieved from the NCBI GenBank database. The alignment has been carried out with MUSCLE [33] and has been visualized and edited using JalView [34].

associated with threonine at position 185, in agreement with previous findings in wine yeast strains [19]. In contrast to wine yeasts, where *IRC7^S* allele is highly abundant [21], *IRC7^L* genotype was the most frequently detected in the brewing strains analyzed in this study. This finding aligns with previous reports by Michel et al. [9] and Krogerus et al. [23], which identified *IRC7^L* as the predominant genotype in *S. cerevisiae* beer strains. The contrasting prevalence of *IRC7* alleles in wine and beer yeasts suggests niche-specific differences in selective pressures associated with fermentation environments and substrate availability. In brewing contexts, the presence of a fully functional *Irc7* enzyme may confer a selective advantage by enhancing the release of volatile thiols from hop-derived cysteinylated and glutathionylated precursors, thereby contributing to desirable aroma complexity. In contrast, in wine fermentation, the low-functioning *Irc7^S* variant leads to elevated intracellular cysteine levels, supporting oxidative stress resistance [21, 42] and the biosynthesis of cysteine-rich copper

metallothioneins such as Cup1, which confer copper tolerance [43]. Under these conditions, the truncated *IRC7^S* allele may be selectively maintained. This trait may be less relevant under brewing conditions, potentially explaining the lower frequency of *IRC7^S* allele in brewing strains. Together, these findings suggest that brewing-associated *S. cerevisiae* strains are genetically enriched in the functional *IRC7^L* allele, supporting its relevance in aroma-driven beer fermentation processes.

3.4 | Assessment of β -Lyase Activity in Brewing Strains

To investigate the relationships between the *IRC7* genotypic diversity and its phenotypic expression, a preliminary assessment of β -lyase activity was performed using BiGGY indicator agar. This medium has been widely employed for the H₂S production screening in yeast [44] and has more recently been proposed as a proxy for identifying yeasts overexpressing *IRC7^L* gene [39].

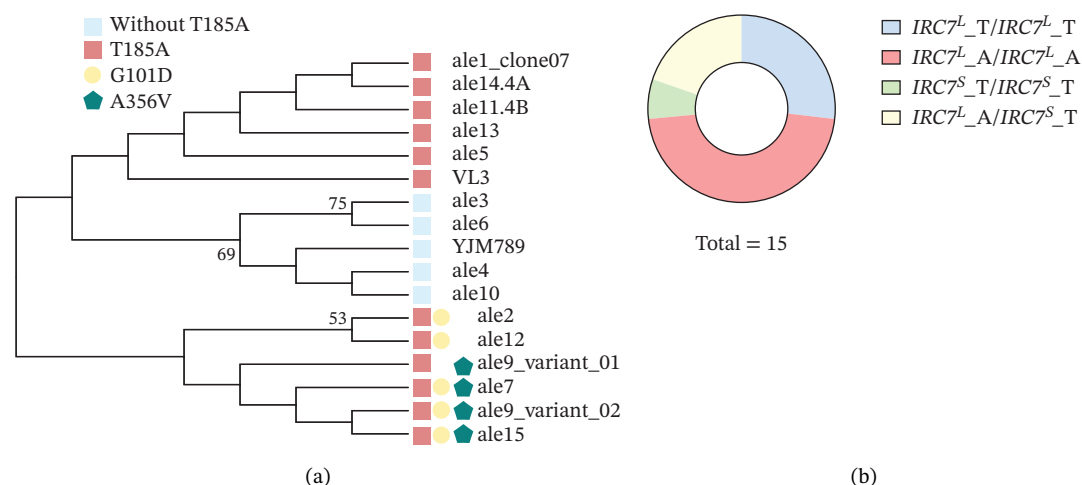


FIGURE 4 | Phylogenetic analysis *Irc7^L* variants and relative abundance distribution of four *IRC7* genotypes in brewing strains. (a) Phylogenetic tree showing the relationship of 15 *Irc7^L* protein sequences among the strains analyzed. *Irc7^L* reference proteins of strains VL3 and YJM789 were used as references. The phylogeny was inferred using maximum likelihood method and WAG model of amino acid substitutions [35]. Bootstrapping was carried out using 100 replicates, and values > 50% are indicated on the nodes. (b) Pie chart illustrates the relative abundance of four different genotypes within the analyzed pool of 15 *S. cerevisiae* ale brewing strains.

Brewing strains were therefore evaluated for H₂S production by comparing colony coloration on BiGGY agar. Notably, intensely dark or reddish colonies were typically observed in most strains with the *IRC7^L/IRC7^L* genotype, regardless of the presence of the T185A substitution (Supporting Figure S4). Some inconsistent results were found for strains ale6, ale12, ale13, and ale15, as well as for an MSC of ale 14 (ale14.4A), which did not grow in BiGGY agar medium despite carrying the *IRC7^L* allele. These results suggested that growth and color development on BiGGY agar are influenced by additional strain-specific physiological factors and should be interpreted cautiously when used as a proxy for β -lyase activity.

To obtain a more quantitative evaluation of β -lyase activity, in vitro enzymatic assays were subsequently performed using three model substrates: L-cysteine, S-ethyl-L-cysteine, and S-methyl-L-cysteine. When L-cysteine was employed as the substrate, the highest enzymatic activity was detected in strain ale7, followed by ale3, ale5, and ale8 (Figure 5(a)). Interestingly, ale8 carries the *IRC7^S* allele with a T at position 185, which would typically be associated with low β -lyase activity. This observation aligns with a previous work [22], in which a brewing strain harboring *IRC7^S* exhibited unexpectedly high activity in vitro L-cysteine-based assays. Together, these observations support the notion that additional enzymes, such as Str3 and Cys3, may

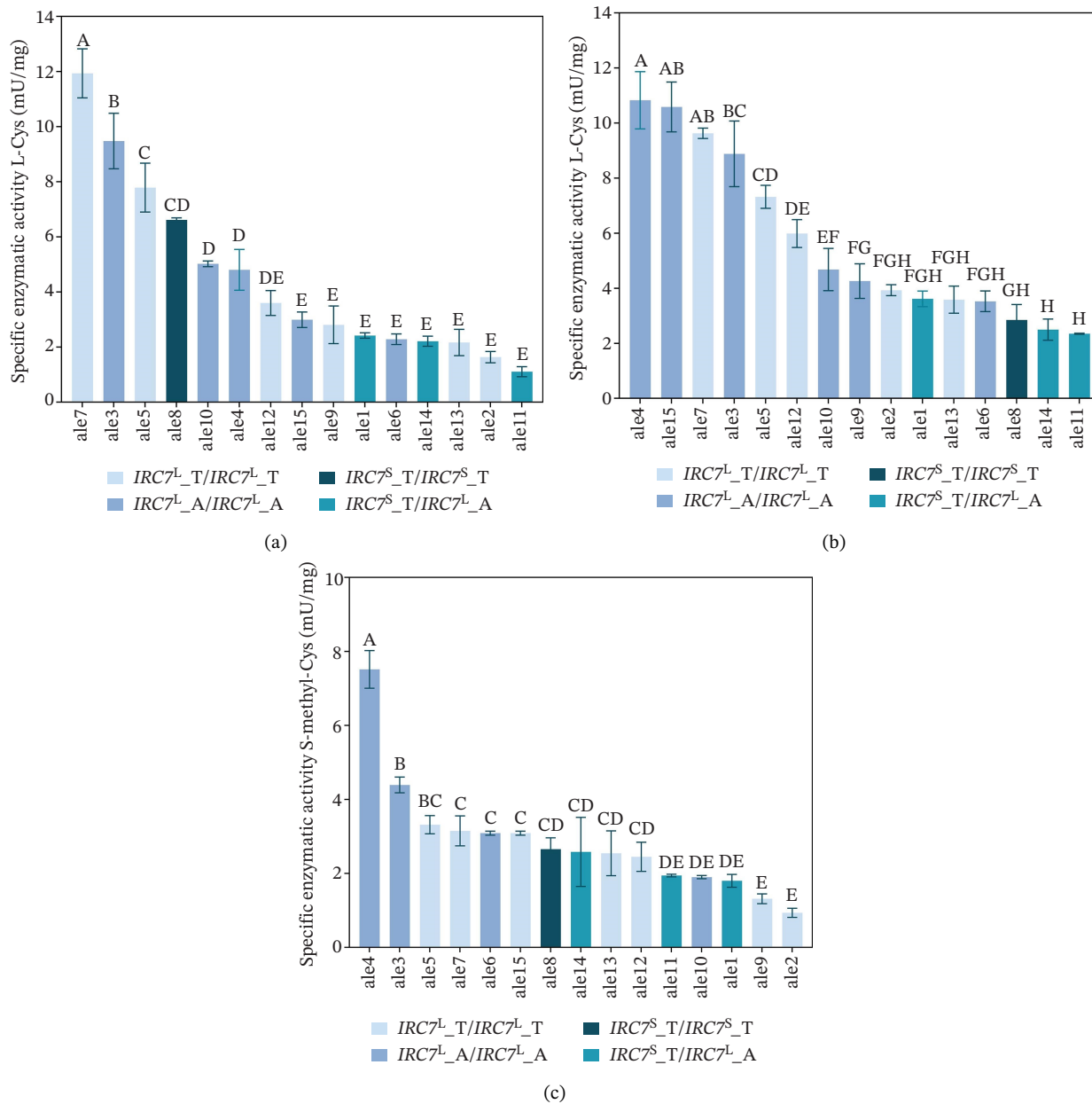


FIGURE 5 | β -Lyase activities of 15 *S. cerevisiae* ale brewing strains measured using (a) L-cysteine (L-Cys), (b) S-ethyl-L-cysteine (S-ethyl-Cys), and (c) S-methyl-L-cysteine S-methyl-Cys) as substrates. Data are expressed as specific enzymatic activity (mU/mg). Values represent the mean of at least three biological replicates; error bars, when visible, indicate standard deviations. Statistical differences were assessed by one-way ANOVA ($p < 0.05$). Different uppercase letters above the bars indicate statistically significant differences. Box colors correspond to the *IRC7* genotype of each strain. Graphs were generated using GraphPad Prism v.10 (GraphPad Software, San Diego, CA, USA).

contribute to cysteine-S-conjugate-lyase activity in *S. cerevisiae*, particularly when simple sulfur-containing substrates are used [45]. In wine yeasts, *Irc7* accounts for the majority of β -lyase activity toward cysteinylated thiol precursors (often > 70%–90% depending on the substrate), whereas *Str3* and *Cys3* display lower catalytic efficiency and narrower substrate specificity, contributing more substantially to activity against simple substrates such as L-cysteine rather than hop- or grape-derived conjugates [8, 15].

Because S-ethyl- and S-methyl-cysteine are structurally more similar to cysteinylated precursors naturally present in malt and hops, these substrates were also employed to better approximate brewing-relevant conditions. Strain ale4 and ale15 exhibited the highest specific enzymatic activity against S-ethyl-cysteine (Figure 5(b)), whereas strain ale4 showed the highest efficiency toward S-methyl-L-cysteine, followed by strain ale3 (Figure 5(c)). Notably, both ale4 and ale3 carried T at position 185 in their *IRC7^L* proteins, suggesting that the presence of threonine at this position may favor β -lyase activity toward certain sulfur-containing substrates.

A comparative analysis of β -lyase activity across multiple substrates was carried out by grouping strains according to the four previously defined genotypes (Figure 6). Overall, heterozygous *IRC7^L/IRC7^S* strains displayed significantly reduced β -lyase activity compared to *IRC7^L/IRC7^L* homozygotes, indicating a negative effect of the truncated allele (Figure 6). When L-cysteine was used as the substrate, heterozygous strains with the *IRC7^S_T/IRC7^L_A* genotype exhibited significantly lower specific enzymatic activity compared to *IRC7^L/IRC7^L* homozygous strains, regardless of the presence of T185A. This finding

suggested that T185A substitution does not impair enzymatic activity against L-cysteine (Figure 6(a)).

In contrast, when S-ethyl-L-cysteine served as the substrate, a marked reduction in β -lyase activity was detected in strains carrying at least one *IRC7^S* allele compared to *IRC7^L/IRC7^L* homozygous strains (Figure 6(b)). For this substrate, the presence of the T85A mutation did not significantly affect the enzyme activity. However, assays using S-methyl-L-cysteine showed that strains with *IRC7^L_T/IRC7^L_T* genotype exhibited the highest β -lyase activity, surpassing that of strains with *IRC7^L_A/IRC7^L_A* genotype (Figure 6(c)). This observation indicates that the T185A substitution can impair β -lyase function in a substrate-depending manner.

Globally, these findings support that both the truncated *Irc7^S* and the T185A substitution negatively influence the β -lyase activity, with the presence of the short allele exerting the most pronounced impact. Importantly, the extent of functional impairment was substrate-dependent, underscoring the complexity of genotype–phenotype relationships in sulfur metabolism. These results were consistent with those previously reported [22] and highlight the importance of considering both allele composition and substrate specificity when evaluating thiol-releasing potential in brewing yeasts. While the in vitro assays employed here provide valuable mechanistic insight into the functional impact of *IRC7* genetic variation, the extent to which these differences translate into volatile thiol release under brewing conditions remains to be validated at the fermentation level as additional external factors such as wort density, oxygen supplementation, nitrogen level, and maturation time have recently been demonstrated to affect the actual release of these thiols [46–48].

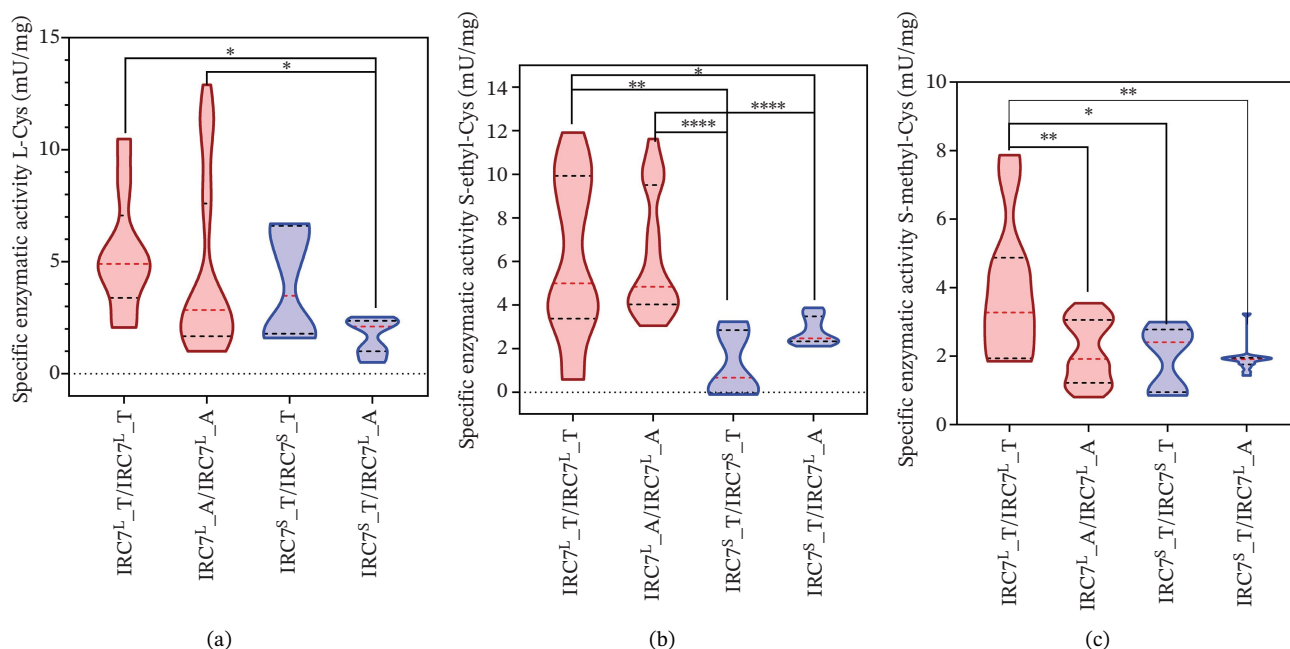


FIGURE 6 | Specific β -lyase activities (expressed as mU/mg) of 15 *S. cerevisiae* ale brewing strains evaluated using (a) L-cysteine (L-Cys), (b) S-ethyl-L-cysteine (S-ethyl-Cys), and (c) S-methyl-L-cysteine (S-methyl-Cys). Strains were categorized according to their *IRC7* genotypes: *IRC7^L_T/IRC7^L_T*, *IRC7^L_A/IRC7^L_A*, *IRC7^S_T/IRC7^S_T*, and *IRC7^L_A/IRC7^S_T*. The red dotted line indicates the median, whereas black dotted lines represent the first and third quartiles. Statistical comparisons among genotypes were performed using the Kruskal–Wallis test ($p \leq 0.05$). Statistical significance is indicated as: *, $p \leq 0.05$; **, $p \leq 0.01$; ***, $p \leq 0.001$; ****, $p \leq 0.0001$. Graphs were generated using GraphPad Prism v.10 (San Diego, CA, USA).

Furthermore, the variability in β -lyase activity observed among strains sharing the same *IRC7* genotype and tested on identical substrates suggests that additional regulatory or genetic factors may contribute to enzymatic diversity. Among these, Str3- and Cys3-mediated activities are likely to play a key role. Str3 has been demonstrated to release polyfunctional thiols from cysteine conjugates [8], while Cys3 releases 2-furfurylthiol from its cysteine conjugate [49]. Although these enzymes generally display lower catalytic efficiency and narrower substrate specificity than *Irc7*, their contribution may partially obscure direct genotype–phenotype relationships based solely on *IRC7* allelic status. In addition, strain-dependent differences in *IRC7* expression levels, potentially driven by variation in the NCR pathway regulation and in other regulatory elements, may further influence β -lyase activity [26, 27]. Elucidation of the relative contribution of these additional β -lyases and regulatory mechanisms will require targeted gene expression and fermentation-based studies, which will be the focus of future investigations.

3.5 | Assessment of β -Lyase Activity in Monosporic Derivatives

To evaluate the functional impact of individual *IRC7* alleles in an isogenic background, β -lyase activity of MSCs derived from heterozygous strains ale14 and ale11 was determined using the three previously described substrates. Specifically, *MATa* MSCs ale14.4A and ale14.7B, derived from ale14, harbored the *IRC7^L_A* and *IRC7^S* variants, respectively, while ale11.4B, a putative *MATa* haploid strain derived from ale11, carried only the *IRC7^L* variant.

For the ale14-derived MSCs, β -lyase activity assays revealed no significant differences in activity between the cultures when L-cysteine was used as the substrate (Figure 7(a)). This result likely reflects the relatively low specificity of L-cysteine for *Irc7* compared to more structurally relevant substrates, as previously observed, and suggests that additional β -lyase enzymes may contribute under these conditions. In contrast, when S-ethyl-L-cysteine was used, ale14.4A (*IRC7^L_A*) displayed increased enzymatic activity relative to the heterozygous parental strain, whereas ale14.7B exhibited a marked reduction in activity, consistent with the presence of the truncated *IRC7^S* variant (Figure 7(a)). These findings indicate that segregation of the functional *IRC7^L* allele can partially restore β -lyase activity toward S-ethyl-L-cysteine in an otherwise heterozygous genetic background.

When S-methyl-L-cysteine was used as the substrate, both MSC derivatives displayed lower β -lyase activity than the parental heterozygous strain, irrespective of the *IRC7* variant present. This observation suggests that β -lyase activity toward this substrate may be influenced by additional genetic or regulatory factors that are disrupted or altered following sporulation. Overall, ale14.7B exhibited the lowest enzymatic activity across all three substrates, followed by the parental ale14 strain and ale14.4A (Figure 7(a)), further supporting the strong negative impact of the *IRC7^S* allele on β -lyase function.

Finally, the MSC ale11.4B, carrying the *IRC7^L_A* variant, displayed a significant increase in β -lyase activity against L-cysteine and S-ethyl-L-cysteine compared to the heterozygous *IRC7^L/IRC7^S* parental strain ale11 (Figure 7(b)). This increase is

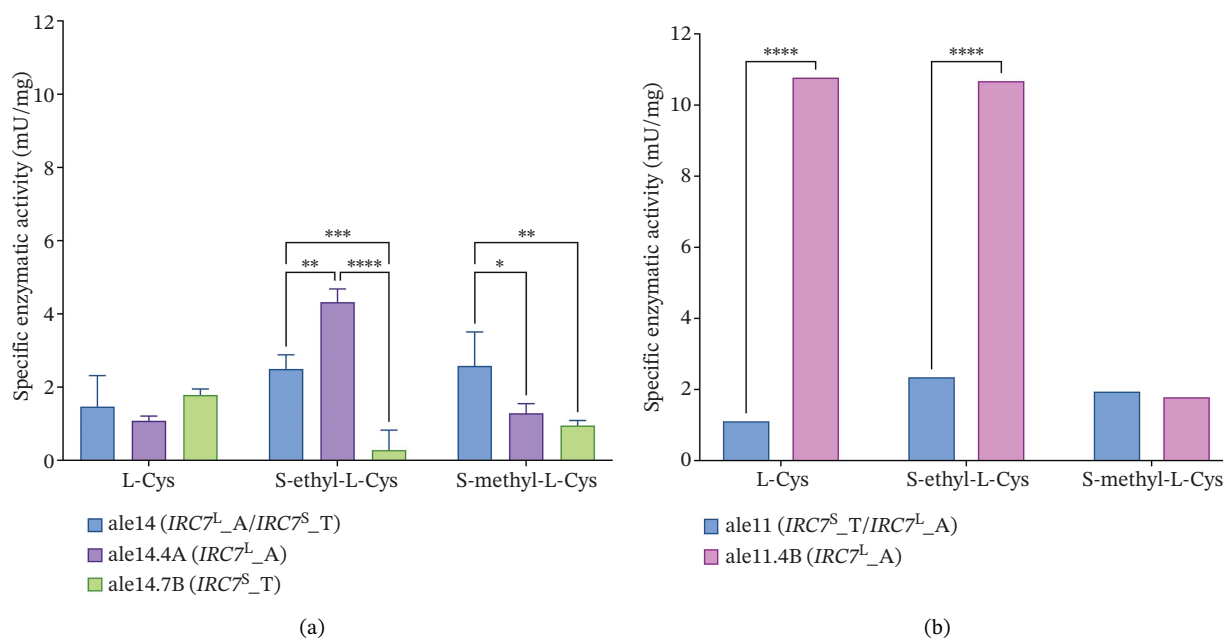


FIGURE 7 | Specific β -lyase activities (mU/mg) of the heterozygous *IRC7^L/IRC7^S* strains ale14 (a) and ale11 (b) and their MSC derivatives assessed using L-cysteine (L-Cys), S-ethyl-L-cysteine (S-Ethyl-L-Cys), and S-methyl-L-cysteine (S-Methyl-L-Cys). Values represent the mean of at least three biological replicates, while error bars indicate standard deviations. Statistical difference was evaluated by one-way ANOVA ($p \leq 0.05$) and is indicated as: *, $p \leq 0.05$; **, $p \leq 0.01$; ***, $p \leq 0.001$; ****, $p \leq 0.0001$. Graphs were generated using GraphPad Prism v.10 (San Diego, CA, USA).

likely to reflect the removal of the truncated *IRC7^S* allele and the resulting exclusive expression of the functional *IRC7^L* variant. In contrast, no significant differences between MSCale11.4B and ale 11 were observed against S-methyl-L cysteine (Figure 6(c)).

4 | Conclusions

This study provides a comparative genotypic and phenotypic characterization of *IRC7* allelic variants across 15 industrial *S. cerevisiae* ale beer strains, offering new insights into the diversity and functional relevance of the *IRC7* gene in the brewing context. In contrast to wine yeasts, where the low-functioning *IRC7^S* allele is prevalent, the majority of brewing strains examined here carried the full-length *IRC7^L* allele, suggesting the action of niche-specific selective pressures likely shaped by fermentation conditions and substrate availability.

Sequencing and phylogenetic analyses revealed high allelic diversity among *IRC7^L* variants, with multiple strains carrying unique combinations of amino acid substitutions, including mutations previously associated with reduced enzymatic activity, such as T185A and G101D. Computational stability predictions and biochemical in vitro assays confirmed that these substitutions differentially impact β -lyase activity in a substrate-dependent mode, thereby modulating the relative thiol-releasing potential relevant to brewing applications. Although fermentation-level validation of thiol production will be addressed in future studies, the present work clearly demonstrated that the T185A substitution in *IRC7^L* affected β -lyase activity toward S-methyl-L-cysteine but not toward L-cysteine or S-ethyl-L-cysteine, whereas the truncated *IRC7^S* allele is generally associated with reduced enzymatic activity across substrates.

Through spore dissection and haplo-selfing, we successfully segregated *IRC7* alleles in heterozygous strains, generating mating-competent MSCs that represent valuable tools for future strain development programs based on breeding. Notably, MSCs carrying only the functional *IRC7^L* allele showed increased β -lyase activity compared to their heterozygous parental strains, further supporting the role of *IRC7^L* in volatile thiol release.

Overall, this study underscores the functional diversity of *IRC7* alleles in brewing yeasts and highlights the potential of genotype-informed selection to enhance thiol-derived aroma production in beer. Moreover, the framework established here provides a foundation for future studies integrating detailed kinetic characterization with fermentation-based validation, enabling a more quantitative understanding of how *IRC7* genetic variation translates into aroma outcomes under brewing conditions.

Author Contributions

C. Nasuti: investigation, data analysis, writing the manuscript, and editing. V. Papiani Ceramelli: conducting the experiment and editing; A. Cattivelli: conducting the experiment and editing; D. Tagliazucchi.: experimental analysis, data curation, and editing. L. Solieri: conceptualization, supervision, visualization, validation, data analysis, writing the manuscript, editing, and funding.

Funding

The project was funded under the National Recovery and Resilience Plan (NRRP), Mission 4 Component 2 Investment 1.4–Call for tender

No. 3138 of December 16, 2021, rectified by Decree n.3175 of December 18, 2021 of the Italian Ministry of University and Research funded by the European Union–NextGenerationEU, Award Number: Project Code CN_00000033, Concession Decree No. 1034 of June 17, 2022 adopted by the Italian Ministry of University and Research, CUP E93C22001090001, Project Title “National Biodiversity Future Center–NBCF.” C.N. was supported by the PhD grant DM n. 352/2022 (CUP E93C22001790004), in the frame of NextGenerationEU PNRR, co-funded by AEB Spa. Open access publishing facilitated by Università degli Studi di Modena e Reggio Emilia, as part of the Wiley - CRUI-CARE agreement.

Conflicts of Interest

The authors declare no conflicts of interest.

Data Availability Statement

Data supporting *IRC7* genotyping are provided as Supporting information. *IRC7* sequences were available under the accession numbers PV876887-PV876904. Data for graphical presentation done using Graph-Pad PRISM V10 software for β -lyase activities are available upon request. Statistical data analysis is available upon request.

References

1. C. Nasuti and L. Solieri, “Yeast Bioflavoring in Beer: Complexity Decoded and Built Up Again,” *Fermentation* 10, no. 4 (2024): 183, <https://doi.org/10.3390/fermentation10040183>.
2. B. Aquilani, T. Laureti, S. Poponi, and L. Secondi, “Beer Choice and Consumption Determinants When Craft Beers are Tasted: An Exploratory Study of Consumer Preferences,” *Food Quality and Preference* 41 (2015): 214–224, <https://doi.org/10.1016/j.foodqual.2014.12.005>.
3. C. T. Hittinger, J. L. Steele, and D. S. Ryder, “Diverse Yeasts for Diverse Fermented Beverages and Foods,” *Current Opinion in Biotechnology* 49 (2018): 199–206, <https://doi.org/10.1016/j.copbio.2017.10.004>.
4. D. Steyer, C. Ambroset, C. Brion, et al., “QTL Mapping of the Production of Wine Aroma Compounds by Yeast,” *BMC Genomics* 13, no. 1 (2012): 573, <https://doi.org/10.1186/1471-2164-13-573>.
5. A. G. Cordente, S. Schmidt, G. Beltran, M. J. Torija, and C. D. Curtin, “Harnessing Yeast Metabolism of Aromatic Amino Acids for Fermented Beverage Bioflavouring and Bioproduction,” *Applied Microbiology and Biotechnology* 103, no. 11 (2019): 4325–4336, <https://doi.org/10.1007/s00253-019-09840-w>.
6. T. Inui, F. Tsuchiya, M. Ishimaru, K. Oka, and H. Komura, “Different Beers With Different Hops. Relevant Compounds for Their Aroma Characteristics,” *Journal of Agricultural and Food Chemistry* 61, no. 20 (2013): 4758–4764, <https://doi.org/10.1021/jf3053737>.
7. N. Rettberg, M. Biendl, and L. A. Garbe, “Hop Aroma and Hoppy Beer Flavor: Chemical Backgrounds and Analytical tools—A Review,” *Journal of the American Society of Brewing Chemists* 76 (2018): 1–20, <https://doi.org/10.1080/03610470.2017.1402574>.
8. S. Holt, M. H. Miks, B. T. de Carvalho, M. R. Foulque-Moreno, and J. M. Thevelein, “The Molecular Biology of Fruity and Floral Aromas in Beer and Other Alcoholic Beverages,” *FEMS Microbiology Reviews* 43, no. 3 (2019): 193–222, <https://doi.org/10.1093/femsre/fuy041>.
9. M. Michel, K. Haslbeck, F. Ampenberger, et al., “Screening of Brewing Yeast β -Lyase Activity and Release of Hop Volatile Thiols from Precursors During Fermentation,” *Brewsci* 72 (2019): 179–186.
10. M. Santiago and R. C. Gardner, “Yeast Genes Required for Conversion of Grape Precursors to Varietal Thiols in Wine,” *FEMS Yeast Research* 15, no. 5 (2015): 609, <https://doi.org/10.1093/femsyr/fov034>.
11. N. Svedlund, S. Evering, B. Gibson, and K. Krogerus, “Fruits of Their Labour: Biotransformation Reactions of Yeasts During Brewery Fermentation,” *Applied Microbiology and Biotechnology* 106, no. 13 (2022): 4929–4944, <https://doi.org/10.1007/s00253-022-12068-w>.

12. K. S. Howell, M. Klein, J. H. Swiegers, et al., "Genetic Determinants of Volatile-Thiol Release by *S. cerevisiae* During Wine Fermentation," *Applied and Environmental Microbiology* 71, no. 9 (2005): 5420–5426, <https://doi.org/10.1128/AEM.71.9.5420-5426.2005>.
13. M. J. Harsch and R. C. Gardner, "Yeast Genes Involved in Sulfur and Nitrogen Metabolism Affect the Production of Volatile Thiols From Sauvignon Blanc Musts," *Applied Microbiology and Biotechnology* 97, no. 1 (2013): 223–235, <https://doi.org/10.1007/s00253-012-4198-6>.
14. S. Holt, A. G. Cordente, S. J. Williams, et al., "Engineering *S. Cerevisiae* to Release 3-Mercaptohexan-1-ol During Fermentation Through Overexpression of *STR3* for Improvement of Wine Aroma," *Applied and Environmental Microbiology* 77, no. 11 (2011): 3626–3632, <https://doi.org/10.1128/AEM.03009-10>.
15. M. Roncoroni, M. Santiago, D. O. Hooks, et al., "The Yeast *IRC7* Gene Encodes a β -Lyase Responsible for Production of the Varietal Thiol 4-Mercapto-4-Methylpentan-2-One in Wine," *Food Microbiology* 28, no. 5 (2011): 926–935, <https://doi.org/10.1016/j.fm.2011.01.002>.
16. J. H. Swiegers and I. S. Pretorius, "Modulation of Volatile Sulfur Compounds by Wine Yeast," *Applied Microbiology and Biotechnology* 74, no. 5 (2007): 954–960, <https://doi.org/10.1007/s00253-006-0828-1>.
17. I. Belda, J. Ruiz, E. Navascués, D. Marquina, and A. Santos, "Improvement of Aromatic Thiol Release Through the Selection of Yeasts With Increased β -Lyase Activity," *International Journal of Food Microbiology* 225 (2016): 1–8, <https://doi.org/10.1016/j.ijfoodmicro.2016.03.001>.
18. P. Darriet, T. Tominaga, V. Lavigne, J.-N. Boidron, and D. Dubourdieu, "Identification of a Powerful Aromatic Component of *Vitis vinifera* Var. Sauvignon Wines: 4-Mercapto-4-Methylpentan-2-One," *Flavour and Fragrance Journal* 10, no. 6 (1995): 385–392, <https://doi.org/10.1002/ffj.2730100610>.
19. A. G. Cordente, A. R. Borneman, C. Bartel, et al., "Inactivating Mutations in *Irc7p* are Common in Wine Yeasts, Attenuating Carbon-Sulfur β -Lyase Activity and Volatile Sulfur Compound Production," *Applied and Environmental Microbiology* 85, no. 6 (2019): e02684–18, <https://doi.org/10.1128/AEM.02684-18>.
20. R. Tofalo, G. Perpetuini, N. Battistelli, F. Tittarelli, and G. Suzzi, "Correlation Between *IRC7* Gene Expression and 4-Mercapto-4-Methylpentan-2-One Production in *S. cerevisiae* Strains," *Yeast* 37, no. 9–10 (2020): 487–495, <https://doi.org/10.1002/yea.3456>.
21. J. Ruiz, M. de Celis, M. Martín-Santamaría, et al., "Global Distribution of *IRC7* Alleles in *S. cerevisiae* Populations: A Genomic and Phenotypic Survey Within the Wine Clade," *Environmental Microbiology* 23, no. 6 (2021): 3182–3195, <https://doi.org/10.1111/1462-2920.15540>.
22. E. A. Vega, "Variation in *Irc7p* Activity Amongst Brewing Strains of *S. cerevisiae*," (Oregon State Univ, 2021), PhD thesis.
23. K. Krogerus, E. Fletcher, N. Rettberg, B. Gibson, and R. Preiss, "Efficient Breeding of Industrial Brewing Yeast Strains Using CRISPR/Cas9-Aided Mating-Type Switching," *Applied Microbiology and Biotechnology* 105, no. 21–22 (2021): 8359–8376, <https://doi.org/10.1007/s00253-021-11626-y>.
24. B. Magasanik and C. A. Kaiser, "Nitrogen Regulation in *S. cerevisiae*," *Gene* 290, no. 1–2 (2002): 1–18, [https://doi.org/10.1016/S0378-1119\(02\)00558-9](https://doi.org/10.1016/S0378-1119(02)00558-9).
25. T. G. Cooper, "Transmitting the Signal of Excess Nitrogen in *S. cerevisiae* From the Tor Proteins to the GATA Factors: Connecting the Dots," *FEMS Microbiology Reviews* 26, no. 3 (2002): 223–238, <https://doi.org/10.1111/j.1574-6976.2002.tb00612.x>.
26. M. Dufour, A. Zimmer, C. Thibon, and P. Marullo, "Enhancement of Volatile Thiol Release of *S. cerevisiae* Strains Using Molecular Breeding," *Applied Microbiology and Biotechnology* 97, no. 13 (2013): 5893–5905, <https://doi.org/10.1007/s00253-013-4739-7>.
27. C. Thibon, P. Marullo, O. Claisse, C. Cullin, D. Dubourdieu, and T. Tominaga, "Nitrogen Catabolic Repression Controls the Release of Volatile Thiols by *Saccharomyces cerevisiae* During Wine Fermentation," *FEMS Yeast Research* 8, no. 7 (2008): 1076–1086, <https://doi.org/10.1111/j.1567-1364.2008.00381.x>.
28. G. Crosato, C. Nadai, M. Carlot, et al., "The Impact of *CUP1* Gene Copy-Number and XVI-VIII/XV-XVI Translocations on Copper and Sulfite Tolerance in Vineyard *Saccharomyces cerevisiae* Strain Populations," *FEMS Yeast Research* 20, no. 4 (2020): foaa028, <https://doi.org/10.1093/femsyr/foaa028>.
29. M. Catallo, F. Iattici, C. L. Randazzo, et al., "Hybridization of *Saccharomyces cerevisiae* Sourdough Strains With Cryotolerant *Saccharomyces bayanus* NBRC1948 as a Strategy to Increase Diversity of Strains Available for Lager Beer Fermentation," *Microorganisms* 9, no. 3 (2021): 514, <https://doi.org/10.3390/microorganisms9030514>.
30. C. S. Hoffman and F. Winston, "A Ten-Minute DNA Preparation From Yeast Efficiently Releases Autonomous Plasmids for Transformation of *Escherichia coli*," *Gene* 57, no. 2–3 (1987): 267–272, [https://doi.org/10.1016/0378-1119\(87\)90131-4](https://doi.org/10.1016/0378-1119(87)90131-4).
31. L. Solieri, O. Antúnez, J. E. Pérez-Ortín, E. Barrio, and P. Giudici, "Mitochondrial Inheritance and Fermentative/Oxidative Balance in Hybrids Between *S. cerevisiae* and *S. uvarum*," *Yeast* 25, no. 7 (2008): 485–500, <https://doi.org/10.1002/yea.1609>.
32. C. Huxley, E. D. Green, and I. Dunham, "Rapid Assessment of *S. cerevisiae* Mating Type by PCR," *Trends in Genetics* 6 (1990): 236, [https://doi.org/10.1016/0168-9525\(90\)90190-H](https://doi.org/10.1016/0168-9525(90)90190-H).
33. R. C. Edgar, "MUSCLE: Multiple Sequence Alignment With High Accuracy and High Throughput," *Nucleic Acids Research* 32, no. 5 (2004): 1792–1797, <https://doi.org/10.1093/nar/gkh340>.
34. A. M. Waterhouse, J. B. Procter, D. M. Martin, M. Clamp, and G. J. Barton, "Jalview Version 2—A Multiple Sequence Alignment Editor and Analysis Workbench," *Bioinformatics* 25, no. 9 (2009): 1189–1191, <https://doi.org/10.1093/bioinformatics/btp033>.
35. S. Whelan and N. Goldman, "A General Empirical Model of Protein Evolution Derived From Multiple Protein Families Using a Maximum-Likelihood Approach," *Molecular Biology and Evolution* 18, no. 5 (2001): 691–699, <https://doi.org/10.1093/oxfordjournals.molbev.a003851>.
36. S. Kumar, G. Stecher, M. Suleski, M. Sanderford, S. Sharma, and K. Tamura, "MEGA12: Molecular Evolutionary Genetics Analysis Version 12 for Adaptive and Green Computing," *Molecular Biology and Evolution* 41, no. 12 (2024): msae263, <https://doi.org/10.1093/molbev/msae263>.
37. E. Capriotti, P. Fariselli, and R. Casadio, "I-Mutant2.0: Predicting Stability Changes Upon Mutation From the Protein Sequence or Structure," *Nucleic Acids Research* 33, no. Suppl. 2 (2005): W306–W310, <https://doi.org/10.1093/nar/gki375>.
38. M. M. Bradford, "A Rapid and Sensitive Method for the Quantitation of Microgram Quantities of Protein Utilizing the Principle of Protein-Dye Binding," *Analytical Biochemistry* 72, no. 1–2 (1976): 248–254, [https://doi.org/10.1016/0003-2697\(76\)90527-3](https://doi.org/10.1016/0003-2697(76)90527-3).
39. M. Santiago and R. C. Gardner, "The *IRC7* Gene Encodes Cysteine Desulphhydrase Activity and Confers on Yeast the Ability to Grow on Cysteine as a Nitrogen Source," *Yeast* 32, no. 7 (2015): 519–532, <https://doi.org/10.1002/yea.3078>.
40. S. J. Hanson and K. H. Wolfe, "An Evolutionary Perspective on Yeast Mating-Type Switching," *Genetics* 206, no. 1 (2017): 9–32, <https://doi.org/10.1534/genetics.116.196905>.
41. L. Solieri, S. Cassanelli, F. Huff, et al., "Insights on Life Cycle and Cell Identity Regulatory Circuits for Unlocking Genetic Improvement in *Zygosaccharomyces* and *Kluyveromyces* Yeasts," *FEMS Yeast Research* 21, no. 8 (2021): foab058, <https://doi.org/10.1093/femsyr/foab058>.

42. E. García-Ríos and J. M. Guillamon, "Mechanisms of Yeast Adaptation to Wine Fermentations," *Progress in Molecular & Subcellular Biology* 58 (2019): 37–59, https://doi.org/10.1007/978-3-030-13035-0_2.
43. C. Gross, M. Kelleher, V. R. Iyer, P. O. Brown, and D. R. Winge, "Identification of the Copper Regulon in *Saccharomyces cerevisiae* by DNA Microarrays," *Journal of Biological Chemistry* 275, no. 41 (2000): 32310–32316, <https://doi.org/10.1074/jbc.m005946200>.
44. A. L. Linderholm, C. L. Findleton, G. Kumar, Y. Hong, and L. F. Bisson, "Identification of Genes Affecting Hydrogen Sulfide Formation in *S. cerevisiae*," *Applied and Environmental Microbiology* 74, no. 5 (2008): 1418–1427, <https://doi.org/10.1128/AEM.02494-07>.
45. Z. Gu, Y. Sun, F. Wu, and X. Wu, "Mechanism of Growth Regulation of Yeast Involving Hydrogen Sulfide From S-Propargyl-Cysteine Catalyzed by Cystathionine- γ -Lyase," *Frontiers in Microbiology* 12 (2021): 679563, <https://doi.org/10.3389/fmicb.2021.679563>.
46. C. Chenot, W. Donck, P. Janssens, and S. Collin, "Malt and Hop as Sources of Thiol S-Conjugates: Thiol-Releasing Property of Lager Yeast During Fermentation," *Journal of Agricultural and Food Chemistry* 70, no. 10 (2022): 3272–3279, <https://doi.org/10.1021/acs.jafc.1c07272>.
47. C. Chenot, E. Thibault de Chanvalon, P. Janssens, and S. Collin, "Modulation of the Sulfanylalkyl Acetate/Alcohol Ratio and Free Thiol Release From Cysteinylated and/or Glutathionylated Sulfanylalkyl Alcohols in Beer Under Different Fermentation Conditions," *Journal of Agricultural and Food Chemistry* 69, no. 21 (2021): 6005–6012, <https://doi.org/10.1021/acs.jafc.1c01610>.
48. A. Gallo, R. Larcher, R. Schneider, et al., "Impact of Oxygen Supplementation During Fermentation on Yeast Gene Expression and Thiol Release in Wine," *Food Microbiology* 133 (2025): 104881, <https://doi.org/10.1016/j.fm.2025.104881>.
49. M. Zha, B. Sun, S. Yin, A. Mehmood, L. Cheng, and C. Wang, "Generation of 2-Furfurylthiol by Carbon-Sulfur Lyase From the Baijiu Yeast *Saccharomyces cerevisiae* G20," *Journal of Agricultural and Food Chemistry* 66, no. 9 (2018): 2114–2120, <https://doi.org/10.1021/acs.jafc.7b06125>.

Supporting Information

Additional supporting information can be found online in the Supporting Information section. (*Supporting Information*)

Table S1. Primers used in this study.

Figure S1. Genotyping of *IRC7^S* and *IRC7^L* alleles in 15 *S. cerevisiae* ale brewing strains. (A) Full-length PCR assay of *IRC7* genes using the primers PF7 and PR8. (B) Nested PCR assay using the internal primers PF2 and PR2. *S. cerevisiae* strain US-05 was used as positive *IRC7^L/IRC7^L* control. Abbreviations: M, DNA ladder used as a molecular size marker. The length of the molecular size marker is in bp.

Figure S2. Cloning of *IRC7^S* and *IRC7^L* alleles from the heterozygous strain ale1. Nested PCR analysis of *E. coli* DH10B clones obtained after transformation with *IRC7* PCR amplicons from strain ale1 yielded nested PCR fragments either of 394 bp, corresponding to the *IRC7^S* variant, or 432 bp, corresponding to the *IRC7^L* variant. Clones selected for subsequent Sanger sequencing are highlighted in red. Strains ale8 and ale9, homozygous for *IRC7^S* and *IRC7^L*, respectively, were included as controls. Abbreviations: M, DNA ladder used as a molecular size marker; fragment sizes are indicated in base pairs (bp).

Figure S3. Alignment of long and short allele protein sequences deduced from *IRC7* PCR amplicons of strain ale1 cloned into pJET1.2 plasmid. The short allele (clone_06) exhibits the premature codon stop, resulting in a truncated *Irc7* protein, whereas the long allele (clone_07) encodes a full-length protein of 400 amino acids. Protein sequence alignment was performed using MUSCLE [1], and the resulting alignment was visualized with JalView [2].

Figure S4. Growth of 15 *S. cerevisiae* ale brewing strains and their derivatives MSCs on BiGGY agar evaluated by drop test. Serial dilutions are indicated on the bottom. Production of H₂S results in a color shift of colonies from white/creamy on YPDA control medium to dark red or brown on BiGGY agar.